



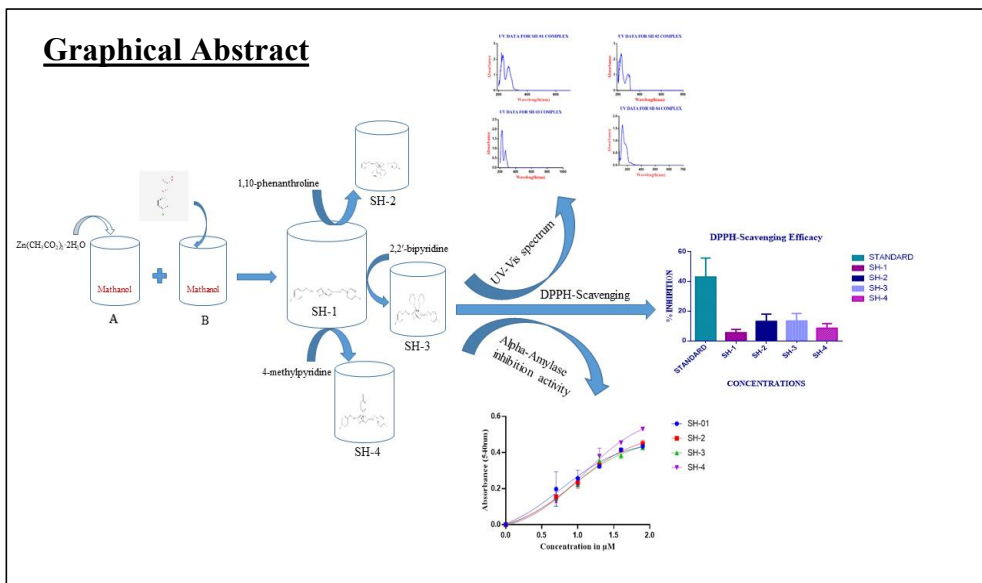
Research Article

Synthesis, characterization and Bioactivity Evaluation of Heteroleptic Zinc(II) Complexes: Antioxidant and α -Amylase Inhibition Studies

Uzair Khan^{1*}, Zeshan Ahmad^{2*}, Sara Ali², Zama Jan³, Murad Khan⁴, Humayun Khan⁵, Sayed Nauman Shah⁶¹School of Chemistry, and Xi'an Key Laboratory of Sustainable Energy Materials Chemistry, Xi'an Jiaotong University, Xi'an 710049, P. R., China.²Department of Chemistry, Abdul Wali Khan University Mardan-3200 Khyber Pakhtunkhwa, Pakistan.³School of Physics, Sustainable Energy & Computational Materials Science, Xi'an Jiaotong University, Xi'an-710049, P. R., China.⁴Department of Chemical Engineering, Faculty of Mechanical, Chemical and Industrial Engineering, University of Engineering and Technology, Peshawar⁵State Key Laboratory of Applied Organic Chemistry, and College of Chemistry and Chemical Engineering, Lanzhou University, Lanzhou 730000, China⁶Department of Chemistry, School of Natural Sciences, National University of Sciences and Technology (NUST), H-12, Islamabad 44000, Pakistan.*Correspondence: (Uzair Khan), uzairxjtu920@stu.xjtu.edu.cn, and (Zeshan Ahmad) zeshanahmad895@gmail.com**Abstract**

A series of four zinc(II) complexes (SH-1 to SH-4) were successfully prepared through the reaction of zinc acetate dihydrate with 4-chlorophenoxyacetic acid (SH-1) in methanol and further reaction with additional ligands (1,10-phenanthroline, 2,2'-bipyridine, and 4-methylpyridine, respectively). The complexes were obtained in satisfactory yields (66-78%) and thoroughly characterized using elemental analysis and atomic absorption spectroscopy, which verified their proposed structure. FT-IR spectral analysis confirmed bidentate chelation of the carboxylate moiety to the zinc center, demonstrating metal-ligand interaction. UV-Visible spectroscopy showed characteristic absorption bands in the 200-300 nm range, corresponding to ligand-centered $\pi \rightarrow \pi^*$ electronic transitions. Biological assessments revealed concentration-dependent antioxidant activity against DPPH radicals and inhibitory effects on α -amylase enzyme, with the 2,2'-bipyridine-containing complex (SH-3) show high performance in both biological assays compared to other complexes. The IC_{50} value of SH-3 is 5.867 ± 0.066 for biological activity. SH-4 shows a higher yield of 78%.

Keywords: Zinc(II) complexes, synthesis, structural characterization, antioxidant activity, enzyme inhibition study

Graphical Abstract**1. Introduction**

Zinc (Zn), a group IIB element of the first transition series, exhibits distinctive chemical properties characterized by its exclusive +II oxidation state. With an electronic configuration of $[Ar]4s^23d^{10}$, Zn^{2+} is redox-inactive yet demonstrates unique chemical behavior among transition metals due to its specific

charge density characteristics. This particular electronic structure and oxidation state confer zinc complexes with notable stability and coordination properties that differ from other transition metal compounds [1]. Zinc demonstrates characteristic Lewis acid behavior, displaying strong binding

affinity toward diverse Lewis base ligands. This metal center commonly adopts stable tetrahedral or octahedral coordination geometries in its complexes, reflecting its versatile coordination chemistry [2]. The human body contains approximately 3 mg of zinc, making it the second most prevalent bio-essential trace metal found in the body [3]. Zinc plays a crucial role in fundamental biological processes and is a vital element in nearly all enzyme categories [4]. "Zinc acts as an effective enzyme inhibitor for multiple enzymes [5]. Moreover, Zinc regulates important physiological functions like cellular recovery from oxidative stress [6-8]. A lack of zinc in the central nervous system can lead to various pathologic issues [9]. Zinc deficiency might lead to the growth of tumors during all stages of tumor development [7]. Figure 1 illustrates several health complications associated with zinc deficiency in humans.

Zinc(II) carboxylate complexes exhibit unique structural diversity and distinctive chemical properties that set them apart from other metal carboxylates. A key feature of these compounds is the versatile coordination behavior of the carboxylate ligand, which can bind to the zinc center in multiple configurations: as a monodentate ligand, in a bridging bidentate mode, or as a chelating bidentate ligand. This remarkable coordination flexibility contributes significantly to the complexes' varied architectures and functional applications in coordination chemistry[10-12]. During this process, the carboxylate ligand may alter its

coordination behavior [9]. The carboxylate shift method produces zinc carboxylate complexes with a variety of geometries, including octahedral, tetrahedral, square pyramidal and trigonal-bipyramidal, in one, two, and three dimensions [13,14]. The bidentate chelators like 1,10-phenanthroline (phen) or 2,2'-bipyridine (bipy) locks part of the zinc coordination sphere. This creates a highly stable, neutral complex unit $[Zn(carboxylate)_2(N-donor)_2]$ or similar. This chelate effect significantly enhances thermal and solution stability compared to complexes with only monodentate ligands coordinated with Zinc, and plays key performance in biological applications.

1.1 Antioxidant

These compounds exhibit antioxidant properties through multiple mechanisms of action against oxidative processes [15, 16]. Living organisms possess an intrinsic antioxidant defense system comprising enzymes such as superoxide dismutase, glutathione peroxidase, and catalase, which work collectively to counteract oxidative stress by neutralizing harmful reactive oxygen species [17]. To prevent free radical-induced oxidation and prolong shelf life, processed food industry routinely employs BHA and BHT as synthetic antioxidant additives in various products) [18, 19]. Key natural antioxidants comprise compounds such as coumarins, carotenoids, flavonoids, tocopherols and others.^[20]

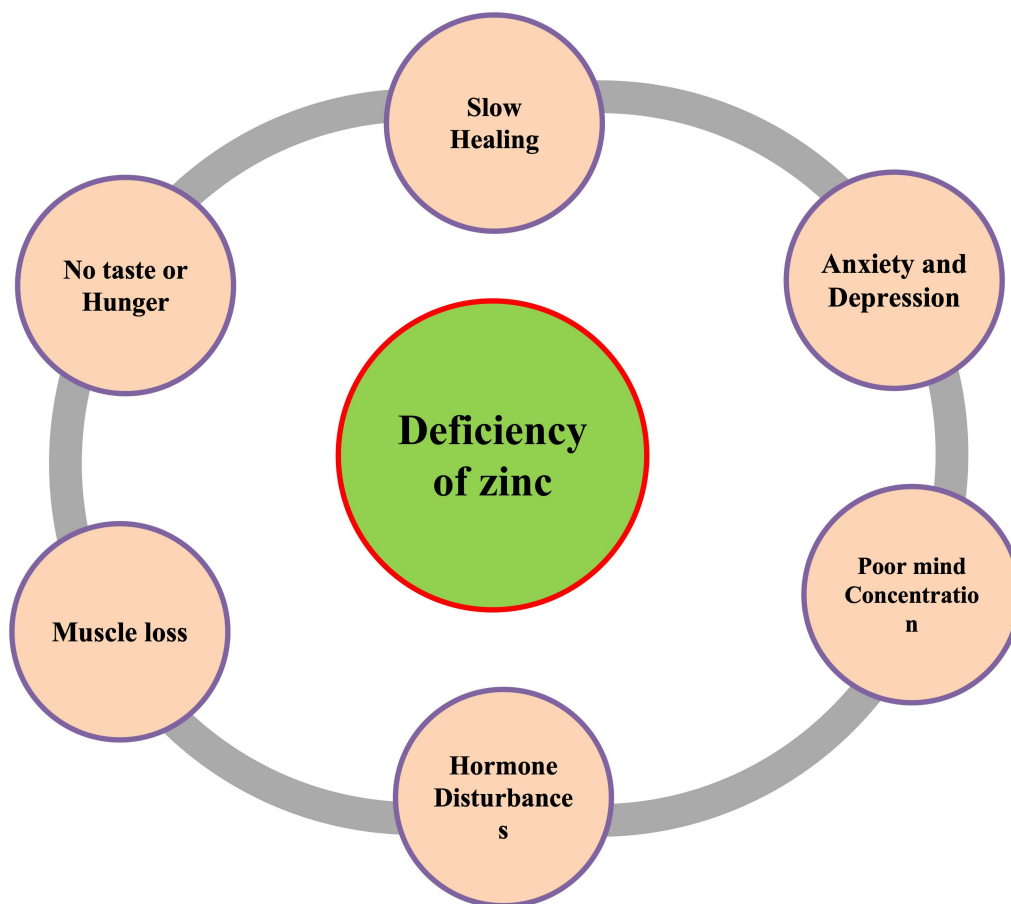


Figure 1. Health disorders resulting from zinc deficiency in humans.

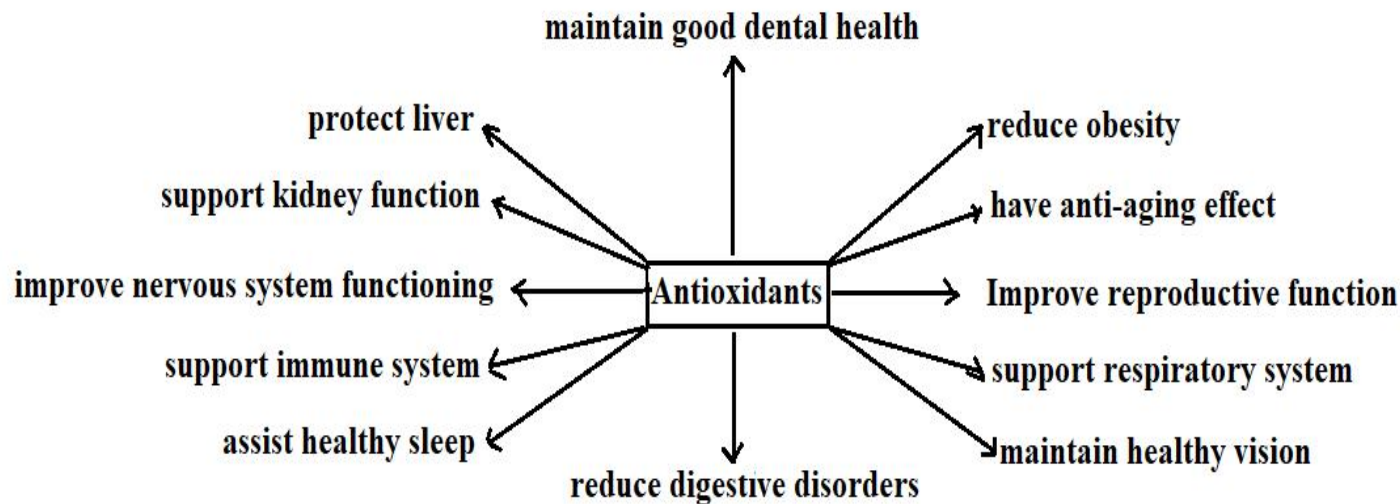


Figure 2. Highlights some of the important beneficial aspects of the antioxidants

1.2 Enzymatic activity

Enzymes bind to their specific substrates in a highly selective manner, enabling these substrates to undergo biochemical transformations at dramatically accelerated rates [21]. Enzyme activity is critically dependent on optimal temperature and pH conditions, with maximal catalytic efficiency occurring at 37°C (normal human body temperature). Activity declines at lower temperatures and is irreversibly lost above 40°C due to thermal denaturation. While enzymes serve as precise biocatalysts in industrial processes, their application faces limitations including narrow reaction specificity, instability in organic solvents, and thermal ability. These challenges have made protein engineering a vibrant research field, focusing on developing novel enzymes with enhanced properties through both natural optimization strategies and in vitro directed evolution approaches [21].

Enzyme inhibition occurs when there is a decline in enzyme-mediated reactions, enzyme synthesis, or catalytic activity. Different classes of enzyme inhibitors can slow down these reaction rates [30].

2. Materials and Methods

2.1. Chemicals reagents

All chemicals and reagents used in this study were of analytical grade and were purchased from Sigma-Aldrich. The antioxidant standard was vitamin C (ascorbic acid). The ligands employed included 4-chlorophenoxyacetic acid, 4-methylpyridine, 2,2'-bipyridine, and 1,10-phenanthroline. The solvents used were methanol, ethanol, and dimethyl sulfoxide (DMSO). Biochemical reagents included α -amylase enzyme, starch, and dinitrosalicylic acid. The free radical species used in the antioxidant assay was DPPH (2,2-diphenyl-1-picrylhydrazyl).

2.2. Instrumentation

The synthesized complexes were characterized using the

following techniques: melting points were determined with a Stuart SMP10 apparatus (UK); FT-IR spectra were recorded using an infrared spectrophotometer; and UV-Vis spectral analyses were carried out on a PerkinElmer UV-Vis spectrophotometer.

2.3. Synthesis of complexes

SH-1. The synthesis was carried out by first dissolving stoichiometric amounts of zinc acetate dihydrate (0.293 g, 1.0 mM) and 4-chlorophenoxyacetic acid (0.5 g, 2.0 mmol) separately in methanol in ratio of 1:2 followed by dropwise addition of the zinc acetate solution to the 4-chlorophenoxyacetic acid solution under constant stirring; the resulting mixture was then heated at 70°C with continuous stirring for 4-5 hours, after completing materials the reaction it was allowed to cool to room temperature and confirmed with TLC which give different spots with the starting materials, after that filtered it to remove methanol and kept it to dry, and left for crystallization under ambient conditions.

SH-2. Complex SH-2 was synthesized following the same initial procedure as SH-1, with the additional step of dropwise addition of 1,10-phenanthroline (0.18 g, 1.0 mmol) (nitrogen donor ligand) into the reaction mixture. The solution was then refluxed for four additional hours before being cooled to room temperature. The product confirmed by TLC and then transferred to a crystallization vessel and allowed to crystallize under ambient conditions, maintaining a 1:2:1 molar ratio of zinc acetate dihydrate, 4-chlorophenoxyacetic acid, and nitrogen donor ligand throughout the synthesis.

SH-3. The synthesis of complex SH-3 followed the same initial protocol as SH-1, with the subsequent addition of 2,2'-bipyridine (0.15 g, 1.0 mmol) (nitrogen donor ligand) via dropwise addition into the reaction mixture. Following a 4-hour reflux period, the solution was cooled to room temperature and transferred to a crystallization vessel for slow evaporation. The reaction maintained strict stoichiometric 1:2:1 molar ratio of zinc acetate dihydrate: 4-

chlorophenoxyacetic acid: 2,2'-bipyridine throughout the synthetic process.

SH-4. The synthesis of complex SH-4 followed the same initial procedure as SH-1. Subsequently, 4-methylpyridine (0.09 g, 1.0 mmol) (nitrogen donor ligand) was added dropwise to the reaction mixture, followed by a 4-hour reflux period. After completion, the solution was cooled to room temperature and transferred to a crystallization vessel.

Table 1. Enzymes and their industrial applications.

Enzyme(s)	Industrial Applications
Cellulases	Biofuel industry: Breaks cellulose into glucose for ethanol fermentation [22].
Proteases, Amylases, Lipases	Detergents: Removes protein, starch, and oil stains from tableware [23]
Amylase, Glucanases, Proteases	Brewing: Degrades polysaccharides and proteins in malt [24].
Beta-Glucanases	Improves beer quality and filtration efficiency [25].
Amyloglucosidase, Pullulanases	Produces low-calorie beer and controls fermentation [25].
Acetolactate Decarboxylase (ALDC)	Enhances fermentation yield by reducing diacetyl production [25].
Papain	Food processing: Tenderizes meat [26].
Lipases	Manufacture of Camembert and blue cheeses [27].
Proteases	Ophthalmology: Cleans proteins from contact lenses to prevent infections [29].
Amylases	Starch industry: Converts starch to glucose and other syrups [30].

The reaction employed stoichiometric ratios of 1:2:1 (zinc acetate dihydrate: 4-chlorophenoxyacetic acid: nitrogen donor ligand) to ensure proper complex formation. The product was then allowed to crystallize under ambient conditions.

2.4. The DPPH-scavenging efficacy of complexes

The antioxidant potential of zinc (II) complexes was evaluated through DPPH radical scavenging assay following a modified Shanab et al. protocol. The experimental procedure involved:

Reaction Setup

Test solutions of the complexes (SH-1 to SH-4) at concentrations ranging from 8 to 64 μM , as well as the standard (ascorbic acid), were mixed with 1 mL of ethanolic DPPH solution (255 μM).

Incubation Conditions

The reaction was carried out in the dark at room temperature for 40 minutes.

Analysis

Absorbance measurements at 517 nm (UV-Vis spectrophotometer)

Triplicate determinations for statistical reliability.

The DPPH radical-scavenging activity can be calculated using the following formula:

$$\text{Inhibition power} = \frac{A_{Con} - A_{Sam}}{A_{Con}} \times 100$$

Where:

A_{con} = Absorbance of the control

A_{sam} = Absorbance of the test sample

2.5. Alpha-Amylase Inhibition Assay

The alpha-amylase inhibitory activity of the synthesized complexes was assessed using a standardized protocol. The assay was performed in 96-well plates with the following reaction mixture:

50- μL phosphate buffer (100 mM, pH 6.8)

10- μL alpha-amylase solution (2 μmL)

20- μL test compound (varying concentrations)

After pre-incubation at 37°C for 20 minutes, 20 μL of 1% starch solution (in phosphate buffer) was added as substrate and incubated for an additional 30 minutes at 37°C. The reaction was terminated by adding 100 μL DNS reagent, followed by heating at for 10 minutes. Absorbance was measured at 540 nm, with acarbose serving as the reference inhibitor at multiple concentrations.

$$\% \text{age Inhibition (\%)} = (1 - A_s/A_c) \times 100$$

Where:

A_s = Abs of sample

A_c = Abs of control

2.6. Statistics of the data

All experimental measurements were performed in triplicate to ensure reproducibility. Statistical analysis was conducted using GraphPad Prism (version 6), employing two key methodologies:

1: Column statistics and linear regression for calculating IC_{50} values with standard error of the mean (SEM)

2: One-way ANOVA to assess significant differences between groups and evaluate variance

The triplicate measurements provided a robust dataset for reliable statistical interpretation of the results.

Table 2. Details of Synthesized complexes SH-1 to SH-4.

(A) Zinc(II)-bis-(4-chlorophenoxy acetate) (SH-1)				(B) Zinc(II)-bis-(4-chlorophenoxy acetate)-N,N-(1,10-phenanthroline) (SH-2)			
Molecular Formula	Molecular	Yield	M.P	Molecular Formula	Molecular	Yield	M.P
C ₁₆ H ₁₀ Cl ₂ O ₆ Zn	434.56	75%	228°C	C ₂₈ H ₁₈ Cl ₂ O ₆ Zn	614.76	66%	142°C
Elemental Composition: Carbon: 44.29% Observed (44.22% theoretical) Hydrogen: 2.37% Observed (2.32% theoretical) FT-IR Spectral Features: 1560 cm ⁻¹ : Strong Asymmetric COO- stretch ($\tilde{\nu}_{as}$) 1467 cm ⁻¹ : Strong symmetric COO- stretch ($\tilde{\nu}_{s}$) $\Delta\tilde{\nu} = 93$ cm ⁻¹ (Indicative of chelating bidentate coordination) 451 cm ⁻¹ : Zn-O vibrational mode Zinc Content (AAS): Measured: 15.02% Calculated: 15.05%				Elemental Analysis (Observed vs Calculated) Carbon: 54.59% (54.70%) Hydrogen: 2.87% (2.95%) Nitrogen: 4.48% (4.56%) FT-IR Spectral signatures: 1593 cm ⁻¹ : Strong COO- stretch ($\tilde{\nu}_{as}$) 1488 cm ⁻¹ : Strong COO- stretch ($\tilde{\nu}_{s}$) $\Delta\tilde{\nu} = 105$ cm ⁻¹ (Chelating bidentate coordination) 724 cm ⁻¹ : Aromatic ring vibration 455 cm ⁻¹ : Zn-O vibrational mode 505 cm ⁻¹ : Zn-N stretching Zinc Content (AAS): Measured: 10.55% Calculated: 10.64%			
(C) Zinc(II)-bis-(4-chlorophenoxy acetate)-N,N-(2,2 bipyridine) (SH-3)				(D) Zinc(II)-bis-(4-chlorophenoxy acetate)-N-4-methylpyridine (SH-4)			
Molecular Formula	Molecular	Yield	M.P	Molecular Formula	Molecular	Yield	M.P
C ₂₆ H ₁₈ Cl ₂ N ₂ O ₆ Zn	590.75	73%	184°C	C ₂₂ H ₁₇ Cl ₂ NO ₆ Zn	527.68	78%	85°C
Elemental Analysis (Observed vs Calculated): Carbon: 52.80% (52.86%) Hydrogen: 3.11% (3.07%) Nitrogen: 4.71% (4.74%) FT-IR Spectral signatures: 1595 cm ⁻¹ : Strong COO- stretch ($\tilde{\nu}_{as}$) 1454 cm ⁻¹ : Strong COO- stretch ($\tilde{\nu}_{s}$) $\Delta\tilde{\nu} = 141$ cm ⁻¹ (Chelating bidentate coordination) 771 cm ⁻¹ : Aromatic ring wagging vibration 461 cm ⁻¹ : Zn-O vibrational mode 506 cm ⁻¹ : Zn-N stretching Zinc Content (AAS): Measured: 11.01% Calculated: 11.07%				Elemental Analysis (Observed vs Calculated): Carbon: 50.01% (50.07%) Hydrogen: 3.31% (3.25%) Nitrogen: 2.61% (2.65%) FT-IR Spectral signatures: 1556 cm ⁻¹ : Strong COO- stretch ($\tilde{\nu}_{as}$) 1423 cm ⁻¹ : Strong COO- stretch ($\tilde{\nu}_{s}$) $\Delta\tilde{\nu} = 133$ cm ⁻¹ (Chelating bidentate coordination) 723 cm ⁻¹ : Aromatic ring wagging vibration 490 cm ⁻¹ : Zn-O vibrational mode 503 cm ⁻¹ : Zn-N stretching Zinc Content (AAS): Measured: 12.36% Calculated: 12.40%			

Note: (A) Zinc(II)-bis-(4-chlorophenoxy acetate) (SH-1); (B) Zinc(II)-bis-(4-chlorophenoxy acetate)-N,N-(1,10-phenanthroline) (SH-2); (C) Zinc(II)-bis-(4-chlorophenoxy acetate)-N,N-(2,2'-bipyridine) (SH-3); and (D) Zinc(II)-bis-(4-chlorophenoxy acetate)-N-(4-methylpyridine) (SH-4), showing molecular formula, molecular weight, yield, melting point, elemental analysis, FT-IR spectral features, and zinc content (AAS).

3. Results and discussions

3.1. FT-IR Results

The FT-IR spectra (4000–400 cm⁻¹) provided crucial insights into the formation and structural features of the zinc(II) carboxylate complexes. This analytical technique confirmed the deprotonation and coordination of the carboxylate ligand, as evidenced by the disappearance of the broad O–H stretching band (3200–2500 cm⁻¹) characteristic of free carboxylic acid. The observed spectral changes verify the conversion of –COOH to carboxylate (COO-) upon complexation with zinc(II). Additionally, the FT-IR data

helped elucidate the binding mode of the carboxylate ligand to the metal center.

The carboxylate ligand's coordination was further verified by Zn-O bond vibrations appearing as weak-medium bands at 490–451 cm⁻¹. Key IR features in metal carboxylates include the asymmetric (ν_a) and symmetric (ν_s) COO- stretches, with their separation ($\Delta\nu$) indicating binding mode. The coordination mode of carboxylate ligands can be determined by their $\Delta\nu$ values:

$\Delta\nu > 250$ cm⁻¹ → Monodentate, $150 < \Delta\nu < 250$ cm⁻¹ → Bridging bidentate, $\Delta\nu < 150$ cm⁻¹ → Chelating bidentate.

The $\Delta\nu$ values of the synthesized complexes (SH-1: 93 cm⁻¹, SH-2: 105 cm⁻¹, SH-3: 141 cm⁻¹, SH-4: 133 cm⁻¹) all fall below 150 cm⁻¹, indicating a chelating bidentate coordination

mode for the carboxylate ligands. For the nitrogen-containing complexes (SH-2, SH-3, SH-4), FT-IR analysis revealed characteristic Zn-N stretching vibrations at 503-506 cm⁻¹ and

strong ring wagging modes at 723-771 cm⁻¹. These spectral features collectively confirm the successful incorporation of ligands in complexes SH-2, SH-3, SH-4.

Table 3. Physicochemical properties of the synthesized complexes.

Complex	Molecular Formula	Molar Mass (g/mol)	Yield (%)	Melting Point (°C)	Solubility Profile
SH-1	C ₁₆ H ₁₀ Cl ₂ O ₆ Zn	434.56	75	228	Methanol, ethanol, acetone, DMSO
SH-2	C ₂₈ H ₁₈ Cl ₂ N ₂ O ₆ Zn	614.76	66	142	Methanol, ethanol, chloroform, DMSO
SH-3	C ₂₆ H ₁₈ Cl ₂ N ₂ O ₆ Zn	590.75	73	184	Methanol, ethanol, chloroform, DMSO
SH-4	C ₂₆ H ₁₇ Cl ₂ NO ₆ Zn	527.68	78	85	Methanol, et

Table 4. Comparative infrared spectral data (cm⁻¹) of the ligand acid and metal complexes.

Vibration Mode	Ligand Acid	SH-1	SH-2	SH-3	SH-4
v(OH) stretch	3500-2500	-	-	-	-
v(C=O) stretch	1703s	-	-	-	-
v(C-O) stretch	1269s	-	-	-	-
v _a (COO ⁻) stretch	-	1560s	1593s	1595s	1556s
v (COO ⁻) stretch	-	1467s	1488s	1454s	1423s
Δv (COO ⁻)	-	93	105	141	133
Aromatic ring wagging	-	-	724	771	723
v(Zn-N) stretch	-	-	505	506	503
v(Zn-O) stretch	-	451	455	461	490

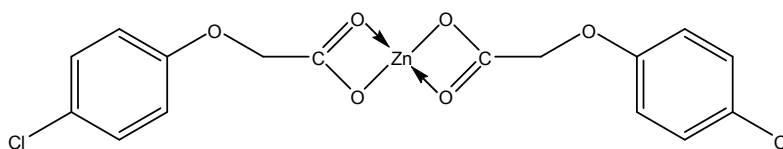


Figure 3. Structure of SH-1.

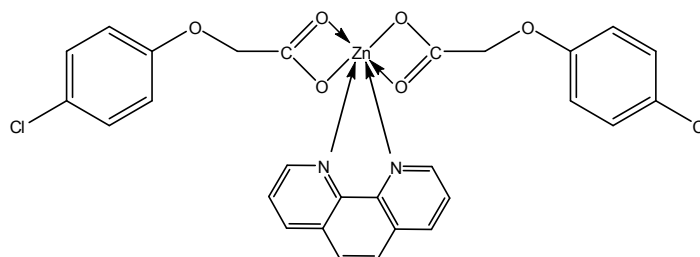


Figure 4. Structure of SH-2.

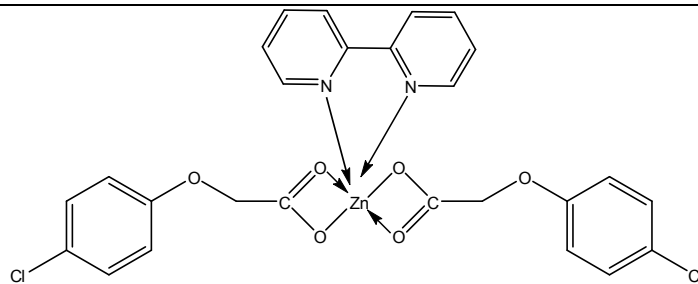


Figure 5. Structure of SH-4.

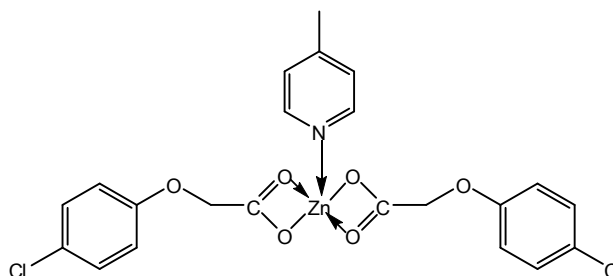


Figure 6. Structure of SH-5.

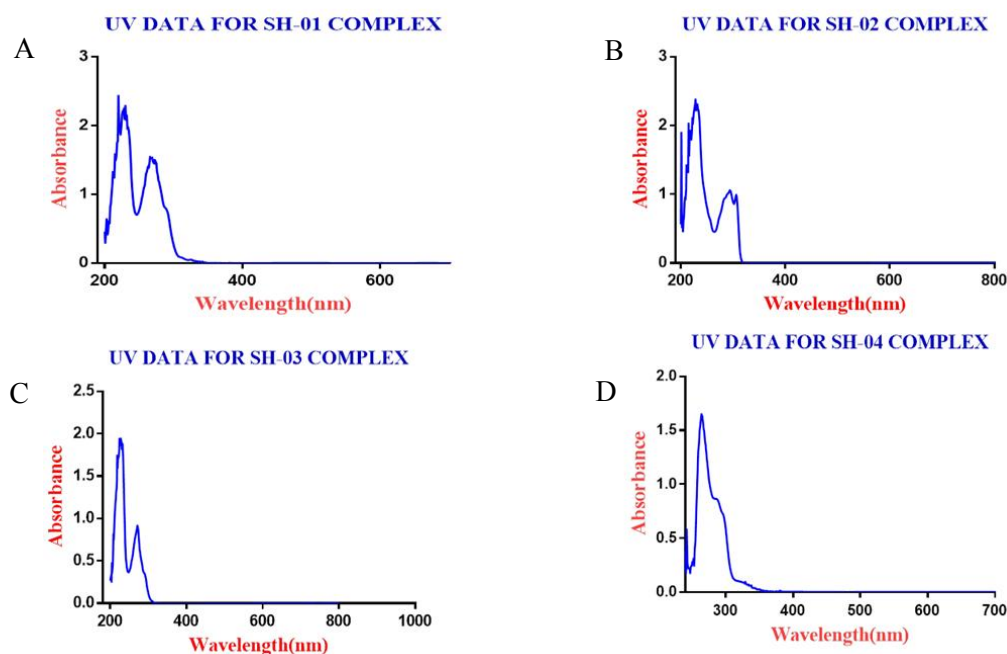


Figure 7. UV-Vis spectra of complexes SH-1 to SH-4. (a) SH-1: Zinc(II)-bis-(4-chlorophenoxy acetate); (b) SH-2: Zinc(II)-bis-(4-chlorophenoxy acetate)-N,N-(1,10-phenanthroline); (c) SH-3: Zinc(II)-bis-(4-chlorophenoxy acetate)-N,N-(2,2'-bipyridine); (d) SH-4: Zinc(II)-bis-(4-chlorophenoxy acetate)-N-(4-methylpyridine).

3.2. Proposed structures of the complexes

FT-IR show the structures proposed for the synthesized complexes are shown in Figures (3-6)

3.3. UV-Vis spectrum

Further characterization of the synthesized complexes was conducted using UV-Vis spectroscopy to examine their

absorption spectra (recorded at 100 μ M in ethanol) displayed in Figures 3.5–3.8. All compounds exhibited distinct absorption bands in the 200–300 nm range, which are likely associated with intra-ligand $\pi \rightarrow \pi^*$ electronic transitions. A slight red shift (bathochromic shift) was observed in the spectra of SH-2, SH-3, and SH-4, possibly due to the extended π -conjugation in their auxiliary ligands (1,10-phenanthroline and 2,2'-bipyridine). This shift suggests that

the aromatic systems of these co-ligands influence the electronic transitions within the complexes

3.4. DPPH-Scavenging efficacy

The DPPH radical scavenging assay is a widely employed method for evaluating the antioxidant activity of compounds, even at low concentrations, due to its sensitivity in detecting free radical-neutralizing potential. When DPPH (a stable free radical) interacts with an antioxidant capable of donating hydrogen atoms (H^+), its characteristic absorbance at 517 nm diminishes. In this study, the DPPH scavenging activity of synthesized Zn(II) complexes was assessed in ethanol and compared with that of ascorbic acid, a standard reference antioxidant. The results help determine the relative antioxidant efficiency of the complexes.

the percentage inhibition of DPPH radicals at varying concentrations of the synthesized Zn(II) complexes shows at Table 5 and Figure 8, revealing a concentration-dependent antioxidant response. The results indicate that higher concentrations of the complexes lead to increased radical scavenging activity. The IC_{50} values listed in Table 3.3 further quantify this effect, showing that while all complexes exhibit dose-dependent antioxidant behavior, their scavenging efficiency remains lower than that of the standard ascorbic acid ($IC_{50} = 102.45 \mu M$). Among the tested complexes, SH-1 displayed the weakest DPPH scavenging ability, highlighting variations in antioxidant potency across the series.

The study revealed notable differences in the DPPH radical scavenging activity of the zinc(II) complexes based on their structural composition. The IC_{50} value for SH-1 (lacking a nitrogen donor ligand) was significantly higher ($823.43 \mu M$),

indicating weaker antioxidant activity. In contrast, complexes SH-2 to SH-4 exhibited lower IC_{50} values (546.87 , 547.34 , and $703.45 \mu M$, respectively), suggesting that the presence of nitrogen donor ligands enhances free radical scavenging potential. SH-2 (1,10-phenanthroline) and SH-3 (2,2'-bipyridine) demonstrated comparable and superior activity compared to SH-4, likely due to their extended aromatic ring systems, which may facilitate better electron delocalization and radical stabilization. This structural feature appears to contribute significantly to their higher antioxidant efficiency, reinforcing the role of aromatic nitrogen donors in enhancing the scavenging activity of zinc(II) carboxylate complexes.

3.5. Alpha-Amylase inhibition activity

Table 6 and Figure 9 illustrate the alpha-amylase inhibition activity of the zinc(II) complexes at varying concentrations. The results demonstrate a concentration-dependent enhancement in enzyme inhibition, with higher concentrations of the complexes leading to increased inhibitory effects. Additionally, the lower IC_{50} values presented in Table 6 indicate greater inhibitory potency of the complexes against the alpha-amylase enzyme. The alpha-amylase inhibition efficacy of the synthesized zinc(II) complexes, determined by their IC_{50} values, follows the order: SH-3 > SH-1 > SH-2 > SH-4. Among these, SH-3 exhibits the strongest inhibitory activity with an IC_{50} value of 5.867 ± 0.066 , while SH-4 demonstrates the weakest inhibition, showing an IC_{50} value of 12.00 ± 0.082 . This trend highlights the varying effectiveness of the complexes in suppressing alpha-amylase activity, with SH-3 being the most potent inhibitor.

Table 5. DPPH Scavenging activity at different concentrations.

Compound	8 μM	16 μM	32 μM	64 μM	128 μM	IC_{50} (μM)
Standard	12.23	20.87	39.09	62.21	81.09	102.45
SH-1	0.9	2.11	5.02	6.31	13.3	823.43
SH-2	2.9	4.02	10.15	20.62	28.22	546.87
SH-3	2.91	4.62	10.19	20.92	28.82	547.34
SH-4	1	3.87	7.76	10.98	19.09	703.45

Table 6. α -Amylase inhibitory activity of synthesized zinc complexes expressed as IC_{50} values.

Compound	$IC_{50} \pm SEM$
SH-1	7.93 ± 0.065
SH-2	9.25 ± 0.069
SH-3	5.867 ± 0.066
SH-4	12.00 ± 0.082

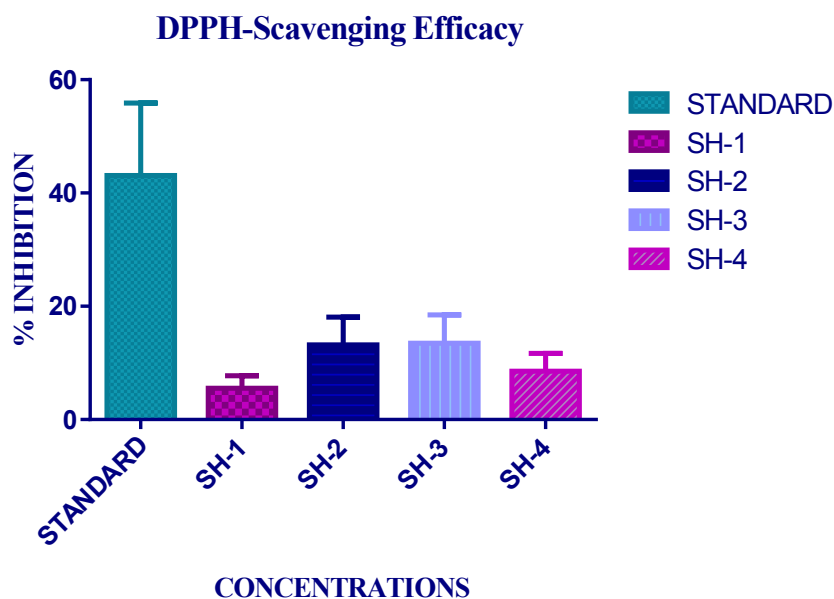


Figure 8. DPPH-Scavenging efficacy of the complexes.

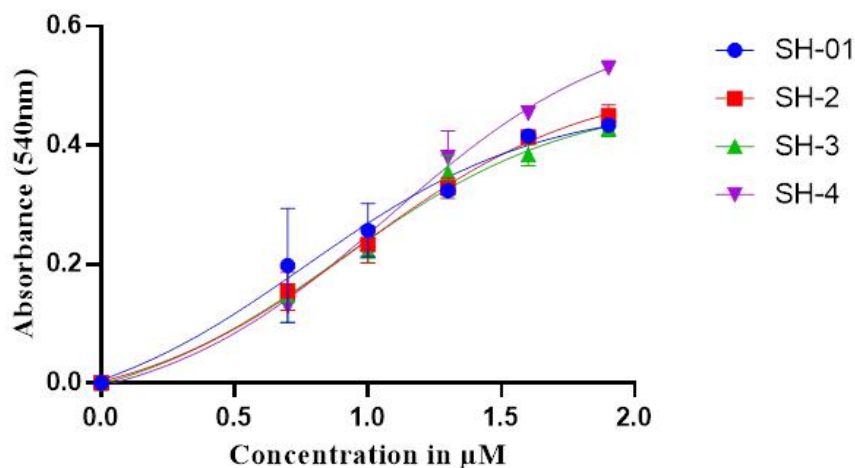


Figure 9. Alpha-amylase inhibition assay of Zinc-complexes.

The outperformance for Bipy could be in luminescence, biological activity, catalytic efficiency and stability. Bipy offers a sweet spot. It provides enough conjugation for strong light absorption and rigidochromism (restriction of motion upon binding), but its slightly less planar and smaller structure reduces detrimental intermolecular π -stacking. This often results in a higher photoluminescence quantum yield (PLQY) for bipy complexes compared to phen analogs, as intermolecular quenching is minimized.

4. Conclusion

A series of zinc(II) complexes (SH1 to SH-4) were prepared by refluxing zinc acetate dihydrate with 4-

chlorophenoxyacetic acid (SH-1) in methanol and further reaction with (1,10-phenanthroline, 2,2'-bipyridine and 4-methylpyridine) ligands. The reactions proceeded efficiently, yielding crystalline products in moderate to good yields (66–78%). Comprehensive characterization through elemental analysis, AAS, FT-IR, and UV-Vis spectroscopic techniques collectively confirmed both the structural and purity of the synthesized complexes. The complexes displayed concentration-dependent antioxidant activity in DPPH radical scavenging assays, with activity trends reflecting the influence of nitrogenous ligands: SH-3 was most active, followed by SH-2, SH-4, and SH-1. In α -amylase inhibition studies, the complexes exhibited varying potency SH-3 was most active,

followed by SH-1, SH-2, and SH-4 suggesting structure-dependent interactions with the enzyme.

Author contributions

Uzair Khan: Uzair Khan: Conceptualization, Methodology, Supervision, Project administration, Writing—original draft. Zeshan Ahmad: Conceptualization, Supervision, Project administration, Investigation, Data curation, Writing—original draft. Sara Ali: Investigation, Data curation, Writing—original draft. Zama Jan: Writing—review & editing. Murad Khan: Investigation, Resources. Humayun Khan: Investigation, Resources. Sayed Nauman Shah: Investigation, Resources. All authors have read and agreed to the published version of the manuscript.

Ethical approval

Not applicable.

Conflicts of Interest

The authors report no conflicts of interest.

Acknowledgment

The authors are thankful to the School of Chemistry and Xi'an Key Laboratory of Sustainable Energy Materials Chemistry, Xi'an Jiaotong University, Xi'an 710049, P. R. China, for providing research facilities and technical support for this work.

Data availability statement

The data presented in this study are available on request from the corresponding author.

Funding

The authors declare that no funds, grants, or other support were received during the preparation of this manuscript.

REFERENCES

1. Zubair, M., et al., Synthesis, physicochemical characterizations and in vitro biological evaluations of amide based Zn (II) carboxylates. *Inorganica Chimica Acta*, 2018. 482: p. 567-578.
2. Ott, I. and R. Gust, Non platinum metal complexes as anti-cancer drugs. *Archiv der Pharmazie: An International Journal Pharmaceutical and Medicinal Chemistry*, 2007. 340(3): p. 117-126.
3. Porkodi, J. and N. Raman, Synthesis, characterization and biological screening studies of mixed ligand complexes using flavonoids as precursors. *Applied Organometallic Chemistry*, 2018. 32(2): p. e4030.
4. Omar, S.N. and H. Abu Ali, New complexes of Zn (II) with the anti-inflammatory non-steroidal drug, ibuprofen and nitrogen donor ligands. Synthesis, characterization and biological activity. *Journal of Coordination Chemistry*, 2017. 70(14): p. 2436-2452.
5. Maret, W., Inhibitory zinc sites in enzymes. *Biometals*, 2013. 26: p. 197-204.
6. Sharif, R., et al., The role of zinc in genomic stability. *Mutation Research/Fundamental and Molecular Mechanisms of Mutagenesis*, 2012. 733(1-2): p. 111-121.
7. Hambidge, K.M. and N.F. Krebs, Zinc deficiency: A special Challenge. *The Journal of nutrition*, 2007. 137(4): p. 1101-1105.
8. Zelenák, V., K. Györyová, and D. Mlynářík, Antibacterial and antifungal activity of zinc (II) carboxylates with/without N-donor organic ligands. *Metal-Based Drugs*, 2002. 8(5): p. 269-274.
9. Bitanirwirwe, B.K. and M.G. Cunningham, Zinc: the brain's dark horse. *Synapse*, 2009. 63(11): p. 1029-1049.
10. Alloway, B.J. (2008) *Zinc in Soils and Crop Nutrition*. 2nd Edition, IZA and IFA, Brussels, Belgium and Paris, France.
11. Benhassine, A., et al., Copper (II) and zinc (II) as metal-carboxylate coordination complexes based on (1-methyl-1H-benzo [d] imidazol-2-yl) methanol derivative: Synthesis, crystal structure, spectroscopy, DFT calculations and antioxidant activity. *Journal of Molecular Structure*, 2018. 1160: p. 406-414.
12. Ullah, K., et al., Designing of homo and heteroleptic zinc (II) carboxylates: synthesis, spectroscopic characterizations, DNA binding study, CTAB interaction and in vitro antimicrobial evaluations. *Journal of the Iranian Chemical Society*, 2019. 16: p. 1163-1177.
13. Wasserscheid, P. and W. Keim, Ionic liquids—new “solutions” for transition metal catalysis. *Angewandte Chemie International Edition*, 2000. 39(21): p. 3772-3789.
14. Jin, S. and D. Wang, *Synthesis and Structural Characterization of Four Zinc Complexes Containing 3, 5-Dimethylpyrazole and Carboxylate Ligands*. 2011, Wiley Online Library.
15. Shahidi, F. and Y. Zhong, Measurement of antioxidant activity. *Journal of functional foods*, 2015. 18: p. 757-781.
16. Gómez, L.J., et al., In-vitro antioxidant capacity and cytoprotective/cytotoxic effects upon Caco-2 cells of red tilapia (*Oreochromis spp.*) viscera hydrolysates. *Food Research International*, 2019. 120: p. 52-61.
17. Beaulieu, M. and H.M. Schaefer, Rethinking the role of dietary antioxidants through the lens of self-medication. *Animal Behaviour*, 2013. 86(1): p. 17-24.
18. Edeas, M., Strategies to target mitochondria and oxidative stress by antioxidants: key points and perspectives. *Pharmaceutical research*, 2011. 28(11): p. 2771-2779.
19. Da Cruz, R.G., et al., Comparison of the antioxidant property of acerola extracts with synthetic antioxidants using an in vivo method with yeasts. *Food chemistry*, 2019. 277: p. 698-705.
20. Shahidi, F., P. Janitha, and P. Wanasundara, Phenolic antioxidants. *Critical reviews in food science & nutrition*, 1992. 32(1): p. 67-103.
21. Hult, K. and P. Berglund, Engineered enzymes for improved organic synthesis. *Current opinion in biotechnology*, 2003. 14(4): p. 395-400.
22. Sun, Y. and J. Cheng, Hydrolysis of lignocellulosic materials for ethanol production: a review. *Bioresource technology*, 2002. 83(1): p. 1-11.
23. Kirk, O., T.V. Borchert, and C.C. Fuglsang, Industrial enzyme applications. *Current opinion in biotechnology*, 2002. 13(4): p. 345-351.
24. Traugott, E.C., From etymology to historical pragmatics. *Topics in English Linguistics*, 2002. 39: p. 19-50.
25. Dulieu, C., et al., Improved performances and control of beer fermentation using encapsulated α -acetolactate decarboxylase and modeling. *Biotechnology progress*, 2000. 16(6): p. 958-965.

26. Tarté, R., Ingredients in meat products: properties, functionality and applications. 2009: Springer.
27. Cakmakci, S., et al., Effect of *Penicillium roqueforti* and incorporation of whey cheese on volatile profiles and sensory characteristics of mould-ripened Civil cheese. *International Journal of Dairy Technology*, 2013. 66(4): p. 512-526.
28. Bajpai, P., Application of enzymes in the pulp and paper industry. *Biotechnology progress*, 1999. 15(2): p. 147-157.
29. Begley, C., S. Paragina, and A. Sporn, An analysis of contact lens enzyme cleaners. *Journal of the American Optometric Association*, 1990. 61(3): p. 190-194.
30. Farris, P. L. (2009). Economic growth and organization of the US corn starch industry. In *Starch* (pp. 11-21). Academic Press.

How to cite this article: Khan, U., Ahmad, Z., Ali, S., Jan, Z., Khan, M., Khan, H., & Shah, S. N. (2026). Synthesis, characterization and Bioactivity Evaluation of Heteroleptic Zinc(II) Complexes: Antioxidant and α -Amylase Inhibition Studies. *Journal of Chemistry and Environment*, 5(1), 1–11.



Copyright © 2026 by the author(s).

Published by Science Research Publishers.

This article is an open-access article distributed under the terms and conditions of the Creative Commons Attribution-NonCommercial-NoDerivatives (CC BY-NC-ND 4.0) License Visit <https://creativecommons.org/licenses/by-nc-nd/4.0/>